Supporting Information for 'Allocating dissipation across a molecular machine cycle to maximize flux'

Aidan I. Brown* and David A. Sivak†
Department of Physics, Simon Fraser University, Burnaby, BC, V5A1S6 Canada

I. OPTIMIZATIONS WITH VARYING NUMBER OF METASTABLE STATES

We investigate the free energy landscape of Fig. 2. For simplicity we set $E_1 - \omega_{\rm tot} = 0$ and hence $E_1 = \omega_{\rm tot}$. The rate constants $k_{12}^{+/-}$ for forward and reverse transitions over the first barrier, with free energy $E_{12}^\ddagger$, are, respectively

$$k_{12}^+ = \tau_{12}^{-1} e^{-(E_{12}^\ddagger - \omega_{\rm tot})} \text{ and } k_{12}^- = \tau_{12}^{-1} e^{-(E_{12}^\ddagger - E_2)} . \quad \text{(S1)}$$

The forward and reverse rate constants over the second barrier, with free energy $E_{21}^\ddagger$, are

$$k_{21}^+ = \tau_{21}^{-1} e^{-(E_{21}^\ddagger - E_2)} \text{ and } k_{21}^- = \tau_{21}^{-1} e^{-E_{21}^\ddagger} . \quad \text{(S2)}$$

The steady-state flux for a two-state cycle is [1]

$$J = \frac{k_{12}^+ k_{21}^+ - k_{12}^- k_{21}^-}{k_{12}^+ + k_{12}^- + k_{21}^+ + k_{21}^-} . \quad \text{(S3)}$$

Inserting Eqs. (S1) and (S2) into (S3) and rearranging gives

$$J = \frac{e^{\omega_{\rm tot}} - 1}{\tau_{12} e^{E_{12}^\ddagger}(1 + e^{-E_2}) + \tau_{21} e^{E_{21}^\ddagger}(1 + e^{\omega_{\rm tot} - E_2})} . \quad \text{(S4)}$$

We consider the states at $E = \omega_{\rm tot}$ and $E = 0$ to be fixed, as varying them relative to one another changes the free energy budget $\omega_{\rm tot}$. We vary E_2, $E_{12}^\ddagger$, and $E_{21}^\ddagger$ to maximize the flux J. Assuming barriers are higher than states, straightforward differentiation shows that

$$\frac{\partial J}{\partial E_{12}^\ddagger} < 0 \text{ and } \frac{\partial J}{\partial E_{21}^\ddagger} < 0 , \quad \text{(S5)}$$

i.e., flux increases as either barrier height decreases. Once the barrier energies are at or below the neighboring state energies, Eqs. (S1) and (S2) no longer hold. Eq. (S5) indicates that the flux is increased by removing the barriers altogether, leaving state 2 (at energy E_2) no longer metastable.

In a separate optimization, we constrain the barriers at fixed energies $E_{12}^\ddagger$ and $E_{21}^\ddagger$, and then vary E_2. Differentiating Eq. (S4), again subject to barriers higher than states, gives

$$\frac{\partial J}{\partial E_2} > 0 , \quad \text{(S6)}$$

meaning that the flux increases as E_2 increases.

The previous two optimizations allowed either the barrier energies to decrease below the neighboring state energies, or E_2 to rise above the barrier energies. We now consider a scenario where the free energy differences $\Delta E_{12}^- = E_{12}^\ddagger - E_2$ and $\Delta E_{21}^+ = E_{21}^\ddagger - E_2$ are fixed, so that E_2, $E_{12}^\ddagger$, and $E_{21}^\ddagger$ move up and down together. This gives rate constants

$$k_{12}^+ = \tau_{12}^{-1} e^{-(E_2 + \Delta E_{12}^- - \omega_{\rm tot})} \quad \text{(S7a)}$$

$$k_{12}^- = \tau_{12}^{-1} e^{-\Delta E_{12}^-} \quad \text{(S7b)}$$

$$k_{21}^+ = \tau_{21}^{-1} e^{-\Delta E_{21}^+} \quad \text{(S7c)}$$

$$k_{21}^- = \tau_{21}^{-1} e^{-(E_2 + \Delta E_{21}^+)} . \quad \text{(S7d)}$$

Substituting these rate constants into Eq. (S3) gives

$$J = \frac{e^{\omega_{\rm tot}} - 1}{e^{E_2}(\tau_{12} e^{\Delta E_{12}^-} + \tau_{21} e^{\Delta E_{21}^+}) + \tau_{12} e^{\Delta E_{12}^-} + \tau_{21} e^{\omega_{\rm tot} + \Delta E_{21}^+}} . \quad \text{(S8)}$$

When barriers are higher than states,

$$\frac{\partial J}{\partial E_2} < 0 , \quad \text{(S9)}$$

meaning the flux increases as E_2 decreases. This continues until one of the barriers is at or below one of the other two states, when Eq. (S7) no longer holds. This optimization, similar to the previous two optimizations, increases the flux by removing the effect of the barriers.

II. ADDITIONAL MODEL DETAILS

We describe our cycles with 'basic' free energy differences ω_{ij} [3, 4], because they directly relate to the ratio of forward and reverse transition rate constants in Eq. (2). Unlike basic free energy differences, 'gross' free energy changes also include the entropic contribution associated with transitions between states with different occupation probabilities [4]. At steady state, the entropic contributions included in the gross free energy cancel out over a complete cycle, making the basic and gross free energy budgets identical.

III. FORWARD LABILE SCHEME

A. Two-state flux

For a two-state cycle, (S3) gives the steady-state flux.

* aidanb@sfu.ca
† dsivak@sfu.ca

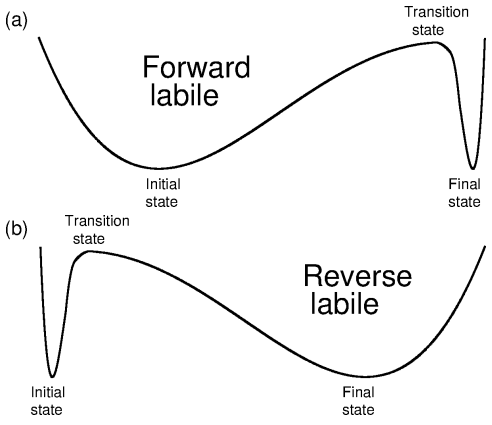

FIG. S1. **Correspondence between energy landscapes and forward and reverse labile schemes.** Forward labile and reverse labile schemes use dissipation to change only forward and reverse rate constants, respectively. In analogy to force-induced unfolding [2], the proximity of the transition state can lead to forward and reverse rates differing in their sensitivity to dissipation. (a) The forward labile scheme corresponds to a transition state quite close to the final state. Changes in the free energy difference between initial and final state (dissipation) lead to a change in the difference between initial and transition states, but not a significant change in the difference between the final and transition states. This changes the forward rate, but not the reverse. (b) Conversely, the reverse labile scheme corresponds to a transition state quite close to the initial state. Dissipation changes lead to relative changes between the final and transition states, but not the initial and transition states. This changes the reverse rate, but not the forward. These two scenarios are extremes; the transition state could be anywhere between the initial and final states.

Each transition has a bare rate constant k_{ij}^0. The log-ratio of the full rate constants is the dissipation ω_{ij} of each transition, $k_{ij}^+/k_{ij}^- = e^{\omega_{ij}}$. For a forward labile scheme, dissipation increases the forward rate constant, $k_{ij}^+ = k_{ij}^0 e^{\omega_{ij}}$, and leaves unchanged the reverse rate constant $k_{ij}^- = k_{ij}^0$ (see main text). With these expressions, the flux can be rewritten as

$$J = \frac{k_{12}^0 k_{21}^0 \left(e^{\omega_{\rm tot}} - 1\right)}{k_{12}^0 \left(e^{\omega_{12}} + 1\right) + k_{21}^0 \left(e^{\omega_{21}} + 1\right)} \ . \tag{S10}$$

We consider reaction cycles with a fixed total free energy dissipation $\omega_{\rm tot} = \omega_{12} + \omega_{21}$. The dissipation allocation is determined by the single free parameter ω_{12}, without loss of generality; the other transition's dissipation $\omega_{21} = \omega_{\rm tot} - \omega_{12}$ is then fixed. Setting $\mathrm{d}J/\mathrm{d}\omega_{12} = 0$ gives

$$\omega_{12}^* = \frac{1}{2}\omega_{\rm tot} + \frac{1}{2}\ln\frac{k_{21}^0}{k_{12}^0} \ . \tag{S11}$$

The corresponding optimal flux is

$$J^* = \frac{k_{12}^0 k_{21}^0 (e^{\omega_{\rm tot}} - 1)}{k_{12}^0 + k_{21}^0 + 2\sqrt{k_{12}^0 k_{21}^0} e^{\omega_{\rm tot}/2}} \ . \tag{S12}$$

To quantify how J/J^* decreases from 1 away from ω_{12}^*, first we solve for J/J^* near ω_{12}^*. Differentiating Eq. (S10) gives

$$\frac{\mathrm{d}J}{\mathrm{d}\omega_{12}} = \frac{k_{12}^0 k_{21}^0 (e^{\omega_{\rm tot}} - 1)(k_{21}^0 e^{\omega_{\rm tot} - \omega_{12}} - k_{12}^0 e^{\omega_{12}})}{(k_{12}^0 + k_{21}^0 + k_{12}^0 e^{\omega_{12}} + k_{21}^0 e^{\omega_{\rm tot} - \omega_{12}})^2} \ . \tag{S13}$$

For $\omega_{12} = \omega_{12}^* + \delta$, expanding to first order in δ produces

$$\frac{\mathrm{d}J}{\mathrm{d}\omega_{12}} \simeq -\left(\frac{1}{2}\frac{k_{12}^0 + k_{21}^0}{\sqrt{k_{12}^0 k_{21}^0}} e^{-\omega_{\rm tot}/2} + 1\right)^{-1} \delta \ . \tag{S14}$$

Integrating and rearranging gives, for small $|\delta| = |\omega_{12} - \omega_{12}^*|$,

$$\frac{J}{J^*} \simeq 1 - \left(\frac{k_{12}^0 + k_{21}^0}{\sqrt{k_{12}^0 k_{21}^0}} e^{-\omega_{\rm tot}/2} + 2\right)^{-1} \delta^2 \ . \tag{S15}$$

For J/J^* far from ω_{12}^*, we divide Eq. (S10) by Eq. (S12),

$$\frac{J}{J^*} = \frac{k_{12}^0 + k_{21}^0 + 2\sqrt{k_{12}^0 k_{21}^0} e^{\omega_{\rm tot}/2}}{k_{12}^0 + k_{21}^0 + k_{12}^0 e^{\omega_{12}} + k_{21}^0 e^{\omega_{\rm tot} - \omega_{12}}} \ . \tag{S16}$$

Rewriting $k_{12}^0 e^{\omega_{12}} = \sqrt{k_{12}^0 k_{21}^0} e^{\omega_{\rm tot}/2} e^{\delta}$ and $k_{21}^0 e^{\omega_{\rm tot} - \omega_{12}} = \sqrt{k_{12}^0 k_{21}^0} e^{\omega_{\rm tot}/2} e^{-\delta}$ gives

$$\frac{J}{J^*} = \frac{k_{12}^0 + k_{21}^0 + 2\sqrt{k_{12}^0 k_{21}^0} e^{\omega_{\rm tot}/2}}{k_{12}^0 + k_{21}^0 + \sqrt{k_{12}^0 k_{21}^0} e^{\omega_{\rm tot}/2}(e^{\delta} + e^{-\delta})} \ . \tag{S17}$$

For large $|\delta| = |\omega_{12} - \omega_{12}^*|$,

$$\frac{J}{J^*} \simeq \left(\frac{k_{12}^0 + k_{21}^0}{\sqrt{k_{12}^0 k_{21}^0}} e^{-\omega_{\rm tot}/2} + 2\right) e^{-|\delta|} \ . \tag{S18}$$

Fig. S2 compares Eqs. (S15) and (S18) to the exact J/J^*, showing good agreement in the expected regimes.

B. Three-state flux for high $\omega_{\rm tot}$

For high total dissipation $\omega_{\rm tot}$, the forward rate constants are exponentially increased, and the backward rate constants are negligible in comparison, producing a cycle with effectively only forward rates. A three-state cycle with only forward rates has steady-state probabilities

$$P_1^{\rm ss} = \left[\left(k_{12}^0\right)^{-1} + \left(k_{23}^0\right)^{-1} e^{\omega_{12} - \omega_{23}} + \left(k_{31}^0\right)^{-1} e^{\omega_{12} - \omega_{31}}\right]^{-1} \ , \tag{S19}$$

with cyclic permutation of states giving $P_2^{\rm ss}$ and $P_3^{\rm ss}$. The resulting steady-state flux is

$$J = \left[\left(k_{12}^0 e^{\omega_{12}}\right)^{-1} + \left(k_{23}^0 e^{\omega_{23}}\right)^{-1} + \left(k_{31}^0 e^{\omega_{31}}\right)^{-1}\right]^{-1} \ . \tag{S20}$$

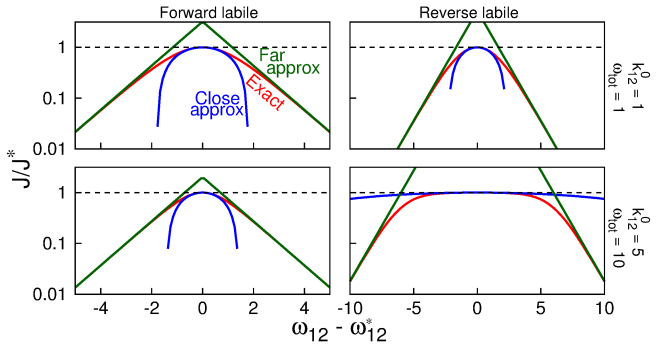

FIG. S2. **Two-state flux sensitivity.** Flux ratio J/J^* as a function of the dissipation allocation, for the two-state cycle with $k^0_{21} = 1$, and k^0_{12} and $\omega_{\rm tot}$ as indicated. For forward labile (reverse labile) cycles, J/J^* is given by Eqs. (S10) and (S12) ((S26) and (S27b)), the close approximation by Eq. (S15) ((S28)), and the far approximation by Eq. (S18) ((S29)). Dashed black line indicates $J/J^* = 1$.

Solving for $\partial J/\partial\omega_{12} = \partial J/\partial\omega_{23} = 0$ gives the optimal allocation

$$\omega^*_{12} = \frac{1}{3}\omega_{\rm tot} + \frac{1}{3}\ln\frac{k^0_{23}k^0_{31}}{(k^0_{12})^2} \ , \tag{S21a}$$

$$\omega^*_{23} = \frac{1}{3}\omega_{\rm tot} + \frac{1}{3}\ln\frac{k^0_{31}k^0_{12}}{(k^0_{23})^2} \ , \tag{S21b}$$

$$\omega^*_{31} = \frac{1}{3}\omega_{\rm tot} + \frac{1}{3}\ln\frac{k^0_{12}k^0_{23}}{(k^0_{31})^2} \ . \tag{S21c}$$

C. Three-state flux for low $\omega_{\rm tot}$

Substituting forward labile rate constants into Eq. (10) and solving for $\partial J/\partial\omega_{12} = \partial J/\partial\omega_{23} = 0$, subject to fixed $\omega_{\rm tot} = \omega_{12} + \omega_{23} + \omega_{31}$, gives

$$e^{2\omega^*_{12}} = k^0_{31}\frac{(k^0_{12})^{-1} + (k^0_{23})^{-1}e^{-\omega^*_{23}}}{1 + e^{\omega^*_{23}}}e^{\omega_{\rm tot}} \ , \tag{S22a}$$

$$e^{2\omega^*_{23}} = \frac{1}{k^0_{23}}\frac{1 + e^{-\omega^*_{12}}}{(k^0_{12})^{-1} + (k^0_{31})^{-1}e^{\omega^*_{12}}}e^{\omega_{\rm tot}} \ . \tag{S22b}$$

For small $\omega_{\rm tot}$, $e^{\omega_{\rm tot}} \simeq 1$, giving

$$e^{2\omega^*_{12}} = k^0_{31}\frac{(k^0_{12})^{-1} + (k^0_{23})^{-1}e^{-\omega^*_{23}}}{1 + e^{\omega^*_{23}}} \ , \tag{S23a}$$

$$e^{2\omega^*_{23}} = \frac{1}{k^0_{23}}\frac{1 + e^{-\omega^*_{12}}}{(k^0_{12})^{-1} + (k^0_{31})^{-1}e^{\omega^*_{12}}} \ . \tag{S23b}$$

Substituting Eq. (S23b) into Eq. (S23a) gives

$$\omega^*_{12} = \frac{1}{2}\ln\frac{k^0_{31}}{k^0_{12}} \ . \tag{S24}$$

Similar derivations yield

$$\omega^*_{23} = \frac{1}{2}\ln\frac{k^0_{12}}{k^0_{23}} \ , \tag{S25a}$$

$$\omega^*_{31} = \frac{1}{2}\ln\frac{k^0_{23}}{k^0_{31}} \ . \tag{S25b}$$

IV. REVERSE LABILE SCHEME

A. Two-state flux

Given rate constants k^+_{ij} and k^-_{ij}, the steady-state flux is Eq. (S3). Substituting reverse labile rate constants $k^+_{ij} = k^0_{ij}$ and $k^-_{ij} = k^0_{ij}e^{-\omega_{ij}}$ gives

$$J = \frac{1 - e^{-\omega_{\rm tot}}}{(k^0_{21})^{-1}\,(1 + e^{-\omega_{12}}) + (k^0_{12})^{-1}\,(1 + e^{-\omega_{21}})} \ . \tag{S26}$$

Solving $\mathrm{d}J/\mathrm{d}\omega_{12} = 0$ subject to fixed $\omega_{\rm tot} = \omega_{12} + \omega_{21}$ gives

$$\omega^*_{12} = \frac{1}{2}\omega_{\rm tot} - \frac{1}{2}\ln\frac{k^0_{21}}{k^0_{12}} \tag{S27a}$$

$$J^* = \frac{1 - e^{-\omega_{\rm tot}}}{(k^0_{12})^{-1} + (k^0_{21})^{-1} + 2(k^0_{12}k^0_{21}e^{\omega_{\rm tot}})^{-1/2}} \ . \tag{S27b}$$

Following similar steps as in Section III A, we find for small $|\delta| = |\omega_{12} - \omega^*_{12}|$,

$$\frac{J}{J^*} \simeq 1 - \left(\frac{k^0_{12} + k^0_{21}}{\sqrt{k^0_{12}k^0_{21}}}e^{\omega_{\rm tot}/2} + 2\right)^{-1}\delta^2 \ , \tag{S28}$$

and for large $|\delta| = |\omega_{12} - \omega^*_{12}|$,

$$\frac{J}{J^*} \simeq \left(\frac{k^0_{12} + k^0_{21}}{\sqrt{k^0_{12}k^0_{21}}}e^{\omega_{\rm tot}/2} + 2\right)e^{-|\delta|} \ . \tag{S29}$$

Fig. S2 compares Eqs. (S28) and (S29) to exact J/J^*, showing good agreement in the expected regimes.

For the two-state cycle, $\omega^{*,\rm FL}_{12} = \omega^{*,\rm RL}_{21}$ and $\omega^{*,\rm FL}_{21} = \omega^{*,\rm RL}_{12}$. This gives

$$\frac{J^{*,\rm FL}_{12+}}{J^{*,\rm FL}_{21-}} = \frac{k^0_{12}}{k^0_{21}}e^{\omega^{*,\rm FL}_{12}} \ , \tag{S30a}$$

$$\frac{J^{*,\rm RL}_{12+}}{J^{*,\rm RL}_{21-}} = \frac{k^0_{12}}{k^0_{21}}e^{\omega^{*,\rm RL}_{21}} \ . \tag{S30b}$$

Substituting $\omega^{*,\rm FL}_{12} = \omega^{*,\rm RL}_{21}$ gives

$$\frac{J^{*,\rm FL}_{12+}}{J^{*,\rm FL}_{21-}} = \frac{J^{*,\rm RL}_{12+}}{J^{*,\rm RL}_{21-}} \ . \tag{S31}$$

Because $\omega^{*,\rm FL}_{12} = \frac{1}{2}\omega_{\rm tot} + \frac{1}{2}\ln(k^0_{21}/k^0_{12})$, the ratios in Eq. (S31) are $\sqrt{k^0_{12}/k^0_{21}}e^{\omega_{\rm tot}/2}$.

B. Three-state flux for high ω_{tot}

Substituting reverse labile rate constants into Eq. (10) and solving for $\partial J/\partial\omega_{12} = \partial J/\partial\omega_{23} = 0$, subject to fixed $\omega_{\mathrm{tot}} = \omega_{12} + \omega_{23} + \omega_{31}$, gives

$$e^{-2\omega_{12}^*} = \frac{1}{k_{12}^0}\frac{1+e^{\omega_{23}^*}}{(k_{23}^0)^{-1}+(k_{31}^0)^{-1}e^{-\omega_{23}^*}}e^{-\omega_{\mathrm{tot}}} \ , \quad \text{(S32a)}$$

$$e^{-2\omega_{23}^*} = k_{31}^0\frac{(k_{23}^0)^{-1}+(k_{12}^0)^{-1}e^{\omega_{12}^*}}{1+e^{-\omega_{12}^*}}e^{-\omega_{\mathrm{tot}}} \ . \quad \text{(S32b)}$$

For high ω_{tot}, these two equations are satisfied by

$$\omega_{12}^* = \frac{1}{3}\omega_{\mathrm{tot}} + \frac{1}{3}\ln\frac{k_{12}^0 k_{31}^0}{(k_{23}^0)^2} \ . \quad \text{(S33)}$$

C. Three-state flux for low ω_{tot}

Approximating $e^{-\omega_{\mathrm{tot}}} \simeq 1$ in Eqs. (S32a) and (S32b) gives

$$e^{-2\omega_{12}^*} = \frac{1}{k_{12}^0}\frac{1+e^{\omega_{23}^*}}{(k_{23}^0)^{-1}+(k_{31}^0)^{-1}e^{-\omega_{23}^*}} \ , \quad \text{(S34a)}$$

$$e^{-2\omega_{23}^*} = k_{31}^0\frac{(k_{23}^0)^{-1}+(k_{12}^0)^{-1}e^{\omega_{12}^*}}{1+e^{-\omega_{12}^*}} \ . \quad \text{(S34b)}$$

Substituting Eq. (S34b) into Eq. (S34a) gives

$$\omega_{12}^* = \frac{1}{2}\ln\frac{k_{12}^0}{k_{23}^0} \ . \quad \text{(S35)}$$

V. EXPERIMENTALLY PARAMETERIZED MODELS

Table S1 shows Hwang and Hyeon's [5] two-state parameterization of the forward and reverse rate constants for catalase, urease, alkaline phosphatase (AP), triose phosphate isomerase (TPI), and kinesin. The dissipation allocation ω_{12} and ω_{21} from these rate constants is compared to the optimal dissipation allocations predicted for forward labile cycles, $\omega_{ij}^{*,\mathrm{FL}}$, and reverse labile cycles, $\omega_{ij}^{*,\mathrm{RL}}$. Fig. 6 summarizes the comparison of experimental fit, forward labile prediction, and even allocation.

For catalase, urease, and AP, the forward labile prediction is quite close to the parameters from [5], while the reverse labile prediction is qualitatively different. For TPI, the forward labile prediction is a very close match to the parameters from [5], but reverse labile prediction is not qualitatively different. For kinesin, neither the forward labile nor reverse labile predictions are clearly a better match for the parameters of [5].

Table S2 shows the three-state parameterization of kinesin from Clancy *et al* [6]. Typical physiological ATP concentrations in the low millimolars [7] motivate the approximation [ATP]$\sim$1mM, giving k_{12}^+, and hence $\omega_{12} \simeq 4$. The second and third transitions are considered 'irreversible,' so we assume that the remaining dissipation budget (from the 20 $k_{\mathrm{B}}T$ free energy provided by ATP hydrolysis) is evenly split to these two transitions, so that $\omega_{23} = \omega_{31} = 8$, providing values for k_{23}^- and k_{31}^-. The forward labile prediction is closer to the parameters from [6] than the reverse labile prediction.

Table S3 shows the four-state parameterization of kinesin from Hwang and Hyeon [5]. k_{12}^+ assumes an ATP concentration of 1mM. Since we do not have quantitative predictions for a four-state cycle, we rank the optimal order for dissipation assigned for a forward labile scheme with more dissipation allocated to smaller reverse rate constants ('First' indicates largest dissipation), and for a reverse labile scheme rank optimal dissipation order by assigning more dissipation to larger forward rate constants. Forward labile predicts the correct ordering of transition dissipations, whereas the reverse labile does not.

	Catalase	Urease	AP	TPI	Kinesin
k_{12}^+	5.8×10^4	1.7×10^4	1.5×10^5	1.7×10^5	2.2×10^3
k_{12}^-	2.2×10^{-13}	7.4×10^{-7}	4×10^{-4}	4.2×10^3	5.5×10^{-1}
k_{21}^+	6.2×10^6	3×10^5	1.6×10^5	1.8×10^5	9.9×10^1
k_{21}^-	6.1×10^6	2.8×10^5	1.4×10^4	1.3×10^4	9.2×10^{-2}
ω_{12}	40	24	20	3.7	8.3
$\omega_{12}^{\mathrm{even}}$	20	12	10	3.2	7.7
$\omega_{12}^{*,\mathrm{FL}}$	42.4	25.3	18.6	3.7	6.6
$\omega_{12}^{*,\mathrm{RL}}$	17.7	6.6	7.5	2.6	9.1
ω_{21}	0.02	0.07	0.13	2.6	7
$\omega_{21}^{\mathrm{even}}$	20	12	10	3.2	7.7
$\omega_{21}^{*,\mathrm{FL}}$	-2.4	-1.3	-1.2	2.6	8.4
$\omega_{21}^{*,\mathrm{RL}}$	22.3	13.4	9.9	3.7	5.9

TABLE S1. **Comparing theoretical predictions and experimental fits of dissipation allocation in two-state enzymatic models**. k_{12}^+, k_{12}^-, k_{21}^+, k_{21}^- are from Table 1 of Hwang and Hyeon [5]. ω_{12} and ω_{21} are calculated using Eq. (2), $\omega_{ij}^{*,\mathrm{FL}}$ using Eq. (8), and $\omega_{ij}^{*,\mathrm{RL}}$ using Eq. (14). Without loss of generality, we adopt the convention that transition 12 is the one with higher dissipation. AP, alkaline phosphatase; TPI, triose phosphate isomerase.

[1] T. Hill, *Free Energy Transduction in Biology: Steady State Kinetic and Thermodynamic Formalism* (Academic Press, 1977).

[2] P. J. Elms, J. D. Chodera, C. Bustamante, and S. Marqusee, Proc. Natl. Acad. Sci. USA **109**, 3796 (2012).

[3] T. Hill and E. Eisenberg, Q. Rev. Biophys. **14**, 463 (1981).

[4] T. Hill, Proc. Natl. Acad. Sci. USA **80**, 2922 (1983).

[5] W. Hwang and C. Hyeon, J. Phys. Chem. Lett. **8**, 250

	12	23	31
k_{ij}^{+}	3000	570	57
k_{ij}^{-}	68	0.2	0.02
ω_{ij}	4	8	8
$\omega_{ij}^{\text{even}}$	6.7	6.7	6.7
$\omega_{ij}^{*,\text{FL}}$	2	7.8	10.1
$\omega_{ij}^{*,\text{RL}}$	6.5	8.8	4.8

TABLE S2. **Comparing theoretical predictions and experimental fits of dissipation allocation in a three-state kinesin model**. k_{12}^{-}, k_{23}^{+}, and k_{31}^{+} are directly from Clancy, *et al* [6] for a three-state main cycle model of mutant kinesin. k_{12}^{+}, k_{23}^{-}, k_{31}^{-}, and ω_{ij} calculated as described in text. $\omega_{ij}^{*,\text{FL}}$ predicted from Eq. (11), $\omega_{ij}^{*,\text{RL}}$ from Eq. (16).

	12	23	34	41
k_{ij}^{+}	3000	600	400	190
k_{ij}^{-}	20	1.4	1.7	120
ω_{ij}	5	6.1	5.5	1.6
$\omega_{ij}^{\text{even}}$	4.6	4.6	4.6	4.6
$\omega_{ij}^{*,\text{FL}}$	Third	First	Second	Fourth
$\omega_{ij}^{*,\text{RL}}$	First	Second	Third	Fourth

TABLE S3. **Comparing theoretical predictions and experimental fits of dissipation allocation in a four-state kinesin model**. All constants except k_{12}^{+} are directly from Hwang and Hyeon's parameterization of a four-state model for kinesin [5]. k_{12}^{+} calculation and ω_{ij}^{*} ranking described in text.

(2017).

[6] B. E. Clancy, W. M. Behnke-Parks, J. O. L. Andreasson, S. S. Rosenfeld, and S. M. Block, Nat. Struct. Mol. Biol. **18**, 1020 (2011).

[7] H. Huang, X. Zhang, S. Li, N. Liu, W. Lian, E. McDowell, P. Zhou, C. Zhao, H. Guo, C. Zhang, C. Yang, G. Wen, X. Dong, L. Lu, N. Ma, W. Dong, Q. P. Dou, X. Wang, and J. Liu, Cell Res. **20**, 1372 (2010).